Surface morphology and electric conductivity of epitaxial Cu(100) films grown on H-terminated Si(100)

E. T. Krastev, L. D. Voice, and R. G. Tobin[a)]
Department of Physics and Astronomy and Center for Fundamental Materials Research, Michigan State University, East Lansing, Michigan 48824-1116

(Received 19 May 1995; accepted for publication 16 January 1996)

We have investigated the crystal structure, surface morphology, and electrical conductance of Cu films grown on H-terminated Si(100). The films were grown by thermal evaporation at 10^{-8} Torr, at deposition rates from 0.1 to 3.5 nm/s and at substrate temperatures from room temperature up to 200 °C. Typical film thicknesses were ~100 nm. Epitaxial growth was verified by x-ray diffraction for films grown near room temperature at rates up to 2 nm/s. The root-mean-square surface roughness was measured to be 1–2 nm using atomic force microscopy (AFM). Higher growth rates or deposition temperatures above 100 °C produced poor quality, nonepitaxial films. Postdeposition annealing at temperatures up to 175 °C did not improve the surface roughness, and at higher annealing temperatures rapid silicide formation destroyed the Cu film. *In situ* electrical resistance measurements and AFM images suggest that for about the first 6 nm of growth the film consists of disconnected islands. X-ray-diffraction data show that the islands consist of crystalline Cu; there is no evidence for a silicide layer. At higher thicknesses the film consists of Cu with an impurity concentration of a few tenths atomic percent. The thickness dependence of the electrical conductance implies a high level of surface, interface, or grain-boundary scattering, characterized by a near-zero apparent specularity parameter p. *© 1996 American Institute of Physics.* [S0021-8979(96)01909-8]

I. INTRODUCTION

Hydrogen-terminated silicon surfaces prepared by wet chemical etching have been shown to be excellent substrates for growing epitaxial films of a variety of fcc and bcc metals.[1–9] In most cases a thin layer of epitaxial copper is used as a seed layer for subsequent growth of other metals. For this reason, and because the low electrical resistivity and large electromigration resistance of copper make it an important technological material,[10] the properties of epitaxial copper films on Si are of particular interest. We report here an investigation of the crystal structure, surface morphology, and electrical conductivity of such films as a function of deposition rate, deposition temperature, and postdeposition annealing. Epitaxial growth is observed over a wide range of deposition conditions. The smoothest films were obtained by near-room-temperature growth at rates of 0.1–1.0 nm/s; higher temperatures and higher deposition rates produced noticeably inferior films. Postdeposition annealing at temperatures up to 125 °C had little effect, while higher temperatures degraded the films.

There have been a number of studies of epitaxial Cu films grown on H-terminated Si,[10–14] but important aspects, including their surface roughness and the nature of the Si–Cu interface, are not yet understood. It has been reported that the films, although epitaxial, are not atomically smooth.[14] There has been no previous systematic investigation of the surface morphology, however, or of the influence of deposition conditions and postdeposition treatment on the morphology. The present work presents such an investigation, together with new information on aspects of film composition and structure that affect electrical transport.

An earlier study[14] revealed the existence of a mixed ''buffer layer'' about 10 nm thick between the Si and the Cu, which is presumably important in facilitating epitaxy. Reflection high-energy electron diffraction (RHEED)[14] and grazing incidence x-ray diffraction[13] studies have shown that the Cu lattice is rotated by 45° relative to the Si lattice, with Cu(010) parallel to Si(011). The rotation reduces the lattice mismatch between the two materials from 40% to 6%. Even a 6% mismatch, however, is unusually large for epitaxial growth. The buffer layer presumably helps to relieve the strain, but its nature—for example, whether it is compositionally disordered or a stoichiometric silicide—has not been established. Our work confirms many of these conclusions, and demonstrates that the buffer layer, although it may contain Si as an impurity, is not a stoichiometric silicide, but is structurally indistinguishable from pure Cu.

Measurements of electrical resistance as a function of thickness during deposition provide additional clues to the quality and composition of the films. The first few nm of the film consist of discontinuous Cu grains. The remainder of the film is relative pure Cu (defect density of a few tenths percent) but with a high level of surface, interface, or grain-boundary scattering that strongly affects film conductance at thicknesses below about 50 nm.

II. FILM STRUCTURE AND SURFACE MORPHOLOGY

The copper films were deposited in a resistive evaporator with base pressure 1×10^{-8} Torr. The (100)Si substrates (B-doped, 20–50 Ω cm resistivity) were prepared by ultrasonic

[a)]Author to whom correspondence should be addressed; Present address: Department of Physics and Astronomy, Tufts University, Medford, MA 02155; Electronic mail: rtobin@tufts.edu

Downloaded¬21¬May¬2008¬to¬130.64.86.72.¬Redistribution¬subject¬to¬AIP¬license¬or¬copyright;¬see¬http://jap.aip.org/jap/copyright.jsp

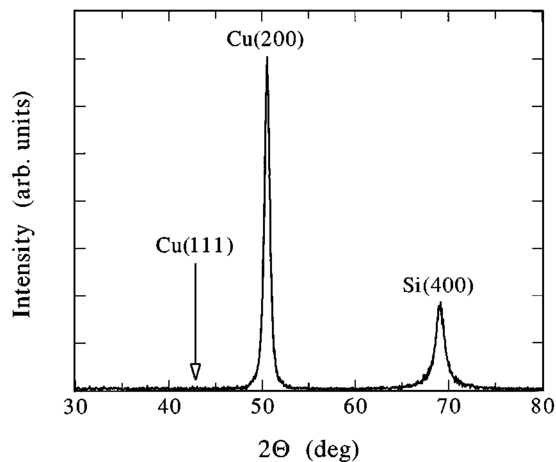

FIG. 1. θ-2θ x-ray-diffraction pattern of 100-nm-thick Cu film deposited on H-terminated Si(100) at 0.1–0.2 nm/s evaporation rate, without intentional heating. The strong Cu(200) peak and absence of a Cu(111) peak indicate highly oriented growth.

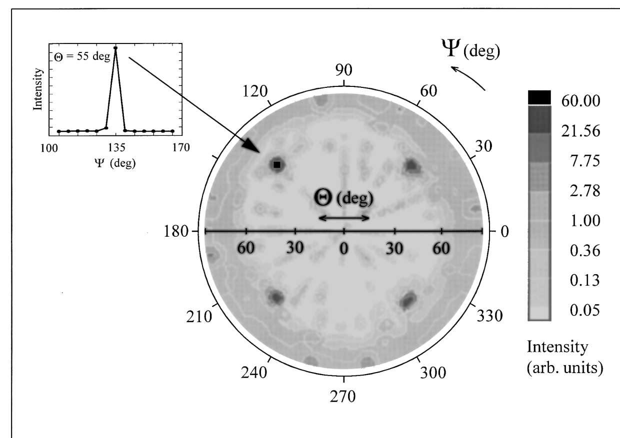

FIG. 2. Cu(111) x-ray pole figure of a 100 nm copper film grown on H-terminated Si(100). Equal areas in the figure represent equal solid angles. The four sharp poles at $\Theta=55°$ demonstrate that the Cu film is epitaxial. The inset shows a scan through one of the poles in the azimuthal Ψ direction keeping the radial angle constant ($\Theta=55°$). The width of the pole is instrument limited.

degreasing with acetone and methanol, etching for 30–60 s in a 10% aqueous solution of HF, and pull drying (slowly and smoothly removing the substrate from the solution with the surface vertical, so that the liquid sheets off smoothly with no droplets). It has been shown that such a procedure leads to an extremely flat and chemically inert surface, with virtually all the Si dangling bonds terminated with H.[15–18] After etching, the samples were loaded into the evaporator and pumping was begun as quickly as possible—within less than 5 min. A pressure of the order of 5×10^{-8} Torr was achieved in about 15 min. The substrates were clamped to a variable-temperature stage so that effects of elevated substrate temperature and postdeposition annealing could be studied. The temperature was measured by a type-K thermocouple mounted on the heating stage, close to the sample. The substrate was not intentionally heated, but the thermocouple on the evaporation stage typically indicated a temperature of 25–30 °C during deposition. The evaporation rate and film thickness were measured using a quartz-crystal monitor calibrated with a diamond stylus profilometer. Most of the films had thicknesses of about 100 nm. During deposition the pressure rose to between 5×10^{-8} and 3×10^{-7} Torr. This is an unusually high pressure for epitaxial growth, and results in a significant impurity concentration in the film, as we discuss below. It is a remarkable feature of the H-terminated Si surface that oriented Cu films can be grown even at pressures of 10^{-4} Torr.[19]

The crystal structure of the films was determined using x-ray diffraction (XRD). The orientation in the direction perpendicular to the surface was characterized by standard θ-2θ scans using Cu $K\alpha$ radiation. Completely disordered (powdered) Cu exhibits a (111) peak 2.17 times more intense than the (200) peak.[20] Polycrystalline Cu films grown on glass, alumina, or oxidized Si substrates typically show a larger (111):(200) ratio, indicating preferential (111) orientation,[13,20] but both peaks are much weaker than the Si(400) peak since only a small fraction of the film volume contributes to each Cu peak. A typical scan of a film grown on an etched (H-terminated) Si(100) substrate is shown in Fig. 1. Highly oriented growth in the direction perpendicular to the surface, with the Cu[100] direction aligned with Si[100], is signaled by a Cu(200) peak at least as strong as the Si(400) peak, and no detectable Cu(111) peak.

The in-plane orientation of our films was determined by means of x-ray pole figures.[21,22] The source-detector angle was set to the Bragg angle for diffraction from Cu(111) planes, and the sample angle was varied over the full range of radial Θ and azimuthal Ψ angles using a four-circle goniometer. Figure 2 shows a Cu(111) pole figure[21] of a 100-nm-thick copper film. The radial angle Θ is the angle between the film normal and the plane of incidence; the azimuthal angle Ψ represents rotation about the surface normal. A completely disordered film would produce a uniform intensity, independent of either angle. A (100) film that was disordered in the plane would exhibit a ring at $\Theta=55°$. The four pronounced Cu(111) poles in Fig. 2 demonstrate that our samples are fully epitaxial. By comparing the integrated intensity in the poles with the background intensity we estimate that >95% of the sample volume is epitaxial. The width of the poles in the azimuthal direction, shown in the inset, is limited by the instrumental resolution. A Si(111) pole figure of the Si substrate was very similar in appearance, except that the four poles were rotated by 45° in Ψ, in agreement with earlier reports that the copper lattice is rotated 45° with respect to the silicon lattice.[13,14]

The surface morphology was studied in air using a commercial atomic force microscope[23] (AFM) with nominal 0.1 nm vertical resolution and 2–5 nm lateral resolution. Most of our scans represent a 1×1 μm^2 area of the surface. The raw topographical images were software processed to eliminate the image bow in the y direction, spurious horizontal stripes, and tilt in the x axis. The primary measure of surface roughness used was the root-mean-square (rms) deviation of the height from the mean. Scans of bare Si substrates yielded rms roughness values of 0.2–0.3 nm.

Downloaded¬21¬May¬2008¬to¬130.64.86.72.¬Redistribution¬subject¬to¬AIP¬license¬or¬copyright;¬see¬http://jap.aip.org/jap/copyright.jsp

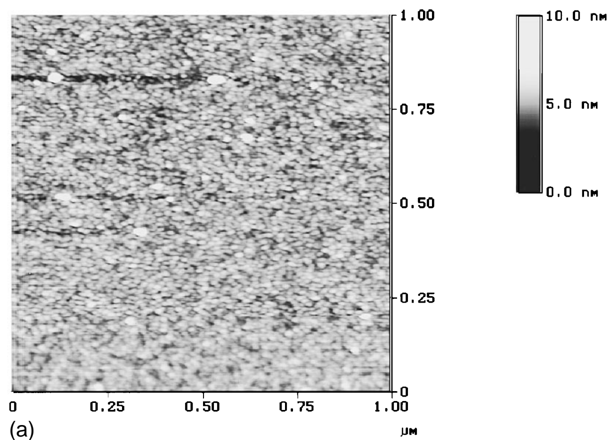

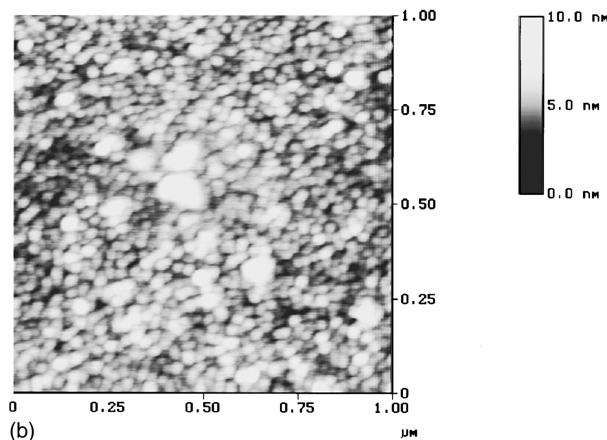

FIG. 3. AFM topographical images of area 1×1 μm^2 for two different film thicknesses; (a) 7.5 nm and (b) 100 nm. The z range from both images is 10 nm and the rms roughness is 0.71 nm for (a) and 0.95 nm for (b). Both films were grown near room temperature and were not annealed.

Figure 3 shows typical AFM images for samples of 7.5 and 100 nm thickness. The deposition rate for both samples was 0.1–0.2 nm/s and the substrate was not intentionally heated. The brightness represents surface height, with brighter areas higher than darker ones, and both images use the same vertical and horizontal scales. Both films exhibit a granular structure, with individual grains 5–10 nm in diameter—comparable to the film thickness—for the 7.5-nm-thick film and 2–3 times larger for the 100 nm film, with a few very large (50 nm) grains. The rms roughness of the thinner film is 0.71 nm versus 0.95 nm for the 100 nm film. Clearly the films, although epitaxial, are rough on the atomic scale. These measurements confirm and quantify the conclusion of Demczyk *et al.*,[14] based on RHEED patterns, that the film growth is three dimensional. On a larger length scale, however, the 100 nm film is relatively smooth, varying in height by a few nm over a lateral distance of tens or hundreds of nm.

XRD from the 7.5-nm-thick film revealed only a distinct Cu(200) peak, as in Fig. 1; there was no evidence of copper silicide peaks. At this thickness the film consists of grains of crystalline copper which are still not fully connected. If there is intermixing of the Cu and Si as reported by Demczyk *et al.*,[14] it does not affect the crystalline structure.

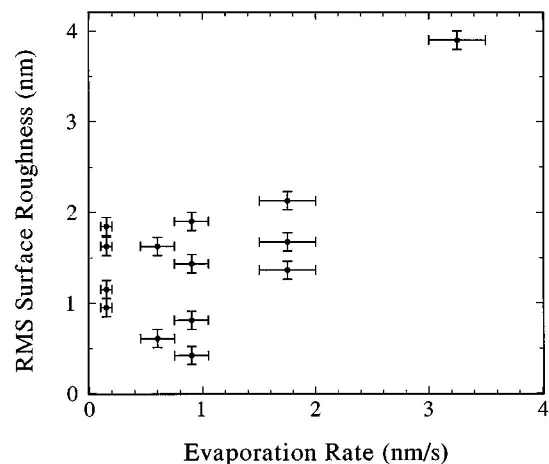

FIG. 4. rms roughness vs deposition rate for 100-nm-thick films grown without intentional heating of the substrate. Each data point represents a 1×1 μm^2 area of a different sample.

We investigated the effect of varying the deposition rate from 0.1 to 3.5 nm/s, without intentional heating of the substrate. All of the films showed good adhesion to the substrate and appeared mirrorlike with the characteristic red color of Cu. X-ray analysis showed strongly oriented growth for deposition rates up to 2 nm/s, but films deposited at 3.0–3.5 nm/s exhibited a Cu(111) peak comparable in intensity to the (200) peak, indicating polycrystalline structure. All of the epitaxial films showed surface morphologies similar to that of Fig. 3(b), and the roughness depended only very weakly on deposition rate. Figure 4 shows rms roughness as a function of deposition rate. For rates up to 1 nm/s the rms roughness is 0.5–2.0 nm; at higher deposition rates the roughness increases to as much as 4 nm.

It is apparent from Fig. 4 that films grown under nominally identical conditions can exhibit significantly different surface roughness. Figure 5 shows an AFM micrograph of a film grown under conditions nominally identical to those

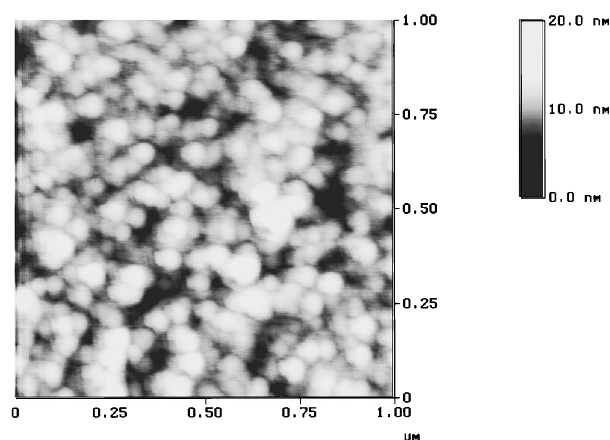

FIG. 5. AFM topographic image of area 1×1 μm^2 of 100 nm Cu film grown under conditions nominally identical to those for the film shown in Fig. 3(b). The z range is 20 nm, and the rms roughness is 1.8 nm. Note the much larger grains and deeper holes.

Downloaded¬21¬May¬2008¬to¬130.64.86.72.¬Redistribution¬subject¬to¬AIP¬license¬or¬copyright;¬see¬http://jap.aip.org/jap/copyright.jsp

TABLE I. Characteristics of 100 nm copper films annealed in vacuum at different temperatures. All of the films were deposited at rates of 0.1–0.2 nm/s, with no intentional heating of the substrate during deposition.

Annealing temperature (°C)	Visual appearance	Crystal structure	Surface morphology	rms roughness (nm)
Not annealed	reddish metal shine, mirrorlike	epitaxial Cu	grains	1–2
125	reddish metal shine, mirrorlike	epitaxial Cu	grains	1–2
150	reddish, cloudy	epitaxial Cu	clusters and holes	2
175	reddish, cloudy	epitaxial Cu	channels	8
200	dull gray-brown	Cu_3Si	not studied	not studied

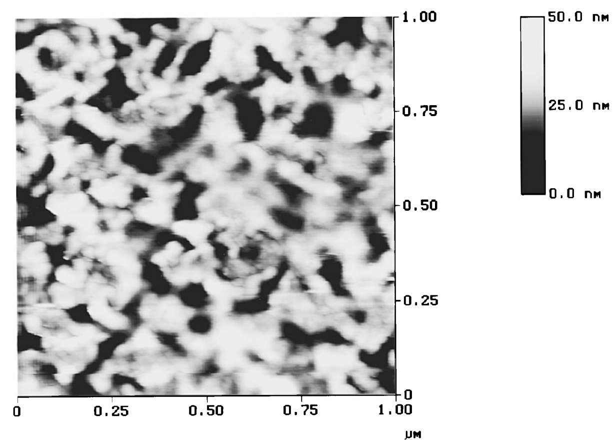

FIG. 6. AFM topographical image of a 100 nm Cu film annealed in vacuum at 175 °C after deposition near room temperature. The z range is 61 nm. The channels penetrate deep into the film, nearly to the Si surface.

used for Fig. 3(b). The lateral scale is the same as in Fig. 3, but the vertical range is twice as great, since the rms roughness of the film in Fig. 5 is 1.82 nm, nearly double that of Fig. 3(b). Much greater coalescence of the crystallites has taken place, leading to larger grains and deeper holes. These variations are perhaps not surprising in view of the high background pressure during deposition. We believe that they arise from uncontrolled variations in the experimental procedure, such as pull-drying technique, time in air before pumpdown, background pressure during deposition, atmospheric humidity, or variations in deposition rate. In the case of Figs. 5 and 3(b), we suspect that the differences are related to atmospheric humidity, which was much higher for the film shown in Fig. 5 than for those shown in Fig. 3. The bulk crystal structure, as revealed by XRD, was insensitive to such variations.

Intentionally heating the substrate during deposition, to temperatures between 100 and 250 °C, resulted in extremely poor films. The films had a dark brown color, and XRD scans showed no peaks attributable to Cu, but a variety of weak peaks similar to those observed by Chang,[12] and attributed to a mixture of Cu_3Si and Cu_4Si. These results agree with the observation of Demczyk *et al.* that substrate temperatures above (or below) room temperature produce inferior films.[14]

We also investigated the effect of postdeposition annealing in vacuum, for films grown near room temperature at deposition rates of 0.1–0.2 nm/s. The results are summarized in Table I. Following deposition the stage was heated to an annealing temperature (125, 150, 175, or 200 °C) over a period of about 15 min. The stage would then be held at the annealing temperature for 15 min and allowed to cool in vacuum for about 8 h before the sample was removed from the evaporator for characterization.

Epitaxial structure was preserved for annealing temperatures up to 175 °C. Films annealed at 125 °C were essentially indistinguishable from unannealed films in surface morphology and roughness. A film annealed at 150 °C exhibited the same rms roughness as an unannealed film, but the AFM images showed the formation of larger copper grains and the appearance of deep holes in the surface. Visually the surface appeared cloudy, as though covered by a whitish haze. These features became more pronounced for films annealed at 175 °C, as shown in Fig. 6. The holes became larger and deeper, extending almost to the surface of the Si (50–60 nm) and forming channel-like structures around the enlarged copper clusters. The rms roughness increased to 8 nm for an annealing temperature of 175 °C.

The picture changed dramatically for the films annealed at 200 °C. Immediately after removal from the evaporator they appeared shiny but gray, and XRD performed within a few hours after removal from vacuum showed only a distinct peak attributable to the (320) planes of Cu_3Si, indicating that the film had reacted completely with the Si. This is in agreement with Chang's observation that the (100) Cu films react rapidly with Si at 200 °C.[12] After the samples annealed at 200 °C were kept in air for one day the color changed to dull gray-brown and instead of the pronounced (320) Cu_3Si peak a larger number of small peaks was detected by XRD. This behavior is consistent with rapid oxidation of the copper silicide at room temperature.

III. ELECTRICAL CONDUCTIVITY

Four-wire dc resistance measurements were made of selected films during deposition. For these samples contact strips (150 nm Ag on top of 10 nm Cr) were deposited on each end of the substrate. The substrate was then removed from the evaporator and etched as described in Sec. II. Some pitting of the silver was observable, but the contacts remained intact. The sample was mounted on the evaporation stage using four phosphor-bronze clips pressing on the contacts, with separate electrical connections for the current and voltage leads. Cu was then deposited at a rate of 0.1–0.4 nm/s to a thickness of 100–400 nm using the procedures described above. The resistance of the film was continuously monitored as a function of film thickness t during the deposition.

Figure 7 shows the apparent film resistivity $\rho(t)$ as a function of t for a typical sample. The resistivity drops rapidly with increasing thickness. The very large range of ρ

Downloaded¬21¬May¬2008¬to¬130.64.86.72.¬Redistribution¬subject¬to¬AIP¬license¬or¬copyright;¬see¬http://jap.aip.org/jap/copyright.jsp

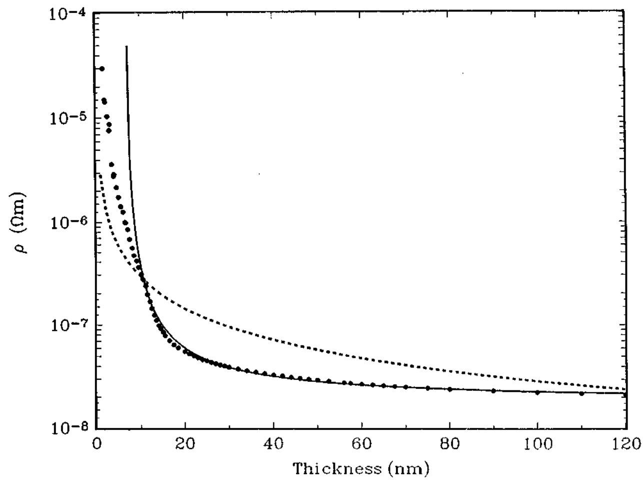

FIG. 7. Apparent resistivity of a Cu film of thickness of $t=120$ nm grown near room temperature at approximately 0.1 nm/s. The dashed line is the best fit to the Fuchs–Sondheimer theory, Eq. (2). The solid line assumes an initial insulating layer of thickness t_0, Eq. (5). The fitting parameters are given.

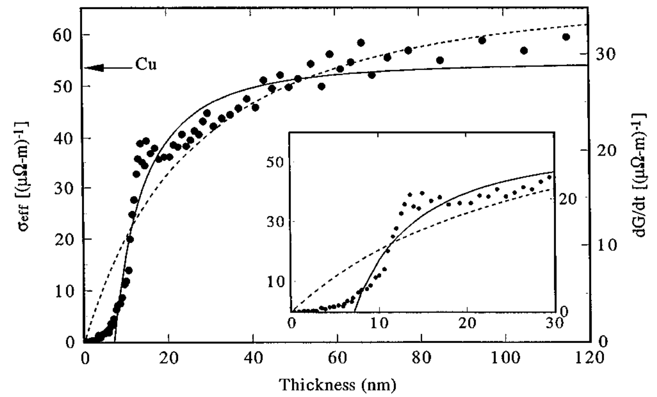

FIG. 8. Effective conductivity $\sigma_{\text{eff}}(t)$ [defined by Eq. (1)] of the same Cu film as in Fig. 7. The dashed line is the best fit to the Fuchs–Sondheimer theory, Eq. (4). The solid line assumes an initial insulating layer of thickness t_0, Eq. (5). The fitting parameters are given. The inset shows the 0–30 nm region on an expanded scale. The arrow indicates the conductivity of pure Cu at the deposition temperature.

values, strong variation with t, uncertainty in the absolute thickness, and non-negligible parallel resistance due to the substrate make it difficult to analyze the data in this form. A more tractable quantity is the conductance derivative $dG(t)/dt$, where $G(t)$ is the conductance of the film at thickness t. This quantity is plotted in Fig. 8 for the same film. It is apparent in Fig. 8, for example, but not in Fig. 7, that little change in conductance occurs for about the first 5 nm. Our use of the conductance derivative is similar to the approach of Fischer, Hoffmann, and Vancea in their study of rough platinum films.[24]

To remove geometrical factors we define an effective conductivity,

$$\sigma_{\text{eff}}(t)=\frac{L}{W}\frac{dG(t)}{dt}, \tag{1}$$

where W and L are the width and length of the film, respectively. In the limit that the thickness is much greater than the electronic mean free path, σ_{eff} can be interpreted as the bulk conductivity of the layer of material at thickness t. For uniform material σ_{eff} should approach the bulk conductivity at large thicknesses, as it does in Fig. 8.

At smaller thicknesses, diffuse scattering of conduction electrons from surface defects and grain boundaries reduces σ_{eff}. The effects of surface scattering are often described within the Fuchs–Sondheimer model of the classical size effect,[24–32] which gives an expression for the effective resistivity of a thin film,

$$\rho(t)=\rho_0\left(1+\frac{\tilde{l}}{t}\right), \tag{2}$$

where ρ_0 is the bulk resistivity of the material, and

$$\tilde{l}=\frac{3}{8}\left(1-\frac{p_v+p_s}{2}\right)l_0 \tag{3}$$

is an effective mean free path, with p_v and p_s the phenomenological specular scattering probabilities at the film–vacuum and film–substrate interfaces, respectively, and l_0 the bulk electron mean free path. Although strictly valid only for $t\gg l_0$, Eq. (2) has been shown to be a good approximation for $t/l_0>0.1$.[29–32] For copper at room temperature $l_0\approx 39$ nm. If the intrinsic conductivity of the deposited material is uniform, the effective conductivity defined by Eq. (1) will have the form

$$\sigma_{\text{eff}}(t)=\sigma_0\left(1-\frac{\tilde{l}^2}{(t+\tilde{l})^2}\right). \tag{4}$$

where σ_0 is the bulk conductivity. Equations (2)–(4) assume plane parallel interfaces, uniform film composition and structure, and thickness-invariant surface scattering. Significant deviations from Eq. (4) would imply that one or more of these assumptions is violated.

The dashed curve in Fig. 8 shows the best fit to Eq. (4), and clearly fails to reproduce the data. Instead of increasing sharply at low t, the data are nearly flat up to about 6 nm. This indicates that the film's resistance does not initially decrease as rapidly as we would expect for a uniform continuous film of copper. Our XRD data for films less than 10 nm thick clearly show that the film consists of crystalline copper and not, for example, a high-resistance silicide. The most likely explanation, consistent with the AFM images, is that at thicknesses less than about 6 nm the film is discontinuous. Similar results were observed for Pt films by Fischer and co-workers.[24] In our measurements some decrease in resistance occurs even at low thicknesses because the presence of the Cu grains decreases the apparent resistance of the Si substrate.

Our goal is to determine whether the basic form of the $\sigma_{\text{eff}}(t)$ curve can be explained by surface scattering, and to estimate the specularity parameter p. Since the detailed form of the curve is rather complex and varied from run to run, we have not attempted a detailed analysis in terms of a roughness parameter, such as was used in Ref. 24. As a first ap-

Downloaded¬21¬May¬2008¬to¬130.64.86.72.¬Redistribution¬subject¬to¬AIP¬license¬or¬copyright;¬see¬http://jap.aip.org/jap/copyright.jsp

proximation, we model the first few nm of the film as an insulating layer of thickness t_0. Subsequent growth of uniform material will then give an effective conductance curve of the form

$$\sigma_{\mathrm{eff}}(t)=\sigma_0\left(1-\frac{\tilde{l}^2}{(t-t_0+\tilde{l})^2}\right), \quad t\geq t_0. \tag{5}$$

The solid line in Fig. 8 shows the best fit of Eq. (5) to the data for $t>8$ nm. The best-fit parameters for this film were

$$\sigma_0=55^{+5}_{-2}\ (\mu\Omega\ \mathrm{m})^{-1},$$
$$\tilde{l}=15^{+5}_{-2}\ \mathrm{nm}, \tag{6}$$
$$t_0=7.0^{+0.5}_{-1.4}\ \mathrm{nm}.$$

Although the model is clearly oversimplified it accounts for the major features of our results. For comparison, the dashed and solid lines in Fig. 7 also show the results of the basic Fuchs–Sondheimer model [Eq. (2)] and the model with an insulating layer of thickness t_0 [Eqs. (5) and (6)].

Several conclusions can be drawn from these results. First, the value of σ_0 is close to that of pure Cu at the deposition temperature, 54 $(\mu\Omega\ \mathrm{m})^{-1}$, and the data are consistent with this value being uniform for $t>8$ nm. Above this thickness, then, the film consists of reasonably pure Cu (see below). Second, the value of $\tilde{l}$ indicates a high level of diffuse scattering. In fact, if Eq. (3) is taken literally we find that the average specularity parameter $p_{\mathrm{avg}}=(p_v+p_s)/2$ is very small or even negative: $-0.37<p_{\mathrm{avg}}<0.11$. Negative p values, while apparently unphysical, have been observed previously[30,33] and indicate a breakdown in the approximations of the Fuchs–Sondheimer theory, notably the assumption of plane parallel surfaces. The AFM images shown here clearly show the inadequacy of this assumption. Nevertheless, if surface scattering is dominant the low value of $\tilde{l}$ shows that the Cu conduction electrons see very rough boundaries at both interfaces. The roughness of the Si/Cu interface may arise from the interdiffusion of Cu and Si as suggested by Demczyk *et al.*[14]

The low value of $\tilde{l}$ could also, however, indicate a high level of internal grain-boundary scattering rather than, or in addition to, scattering from rough interfaces. Scattering from internal defects is normally assumed to be independent of thickness, but in thin film growth the grain size often increases with t, as our AFM images suggest. In that case grain-boundary scattering can give a thickness-dependent resistivity that closely approximates Eq. (2).[28,29,34] Our data cannot distinguish between these mechanisms.

The absolute value of the bulk conductivity σ_0 depends upon knowledge of the geometrical factor L/W. To verify the absolute average conductivity of the finished films, we cleaved the samples to remove the silver contacts and attached wires to the four corners with indium solder. This configuration permits a geometry-independent determination of the film conductivity.[35] Measurements were made both at room temperature and at 4.2 K. The room-temperature conductivities of the films ranged from 48 to 56 $(\mu\Omega\ \mathrm{m})^{-1}$, consistent with the *in situ* measurements.

Residual resistivity ratios [$(R300\ \mathrm{K})/R(4.2\ \mathrm{K})$, where $R(T)$ is the resistance of the film at temperature T] of the films ranged from 5.25 to 6.65, giving low-temperature conductivities of about 320 $(\mu\Omega\ \mathrm{m})^{-1}$. From this value we can very roughly estimate a defect or impurity density on the order of 0.3%. Possible types of defect are chemical impurities, grain boundaries, and lattice defects caused by the strain from the 6% mismatch[13] between the Si and Cu lattices. We suggest that impurities incorporated from background gas during growth are a significant source of low-temperature resistance. At the growth rates used, the flux of background gas on the sample was about 5–30% of the Cu flux, so incorporation of even 1% of the incident impurities could account for the observed resistivity. A higher resistivity ratio (at least 10) was reported for films grown by a different technique in ultrahigh vacuum (10^{-10} Torr),[10] which suggests that the impurity flux can have a significant effect on the low-temperature resistivity.

IV. CONCLUSIONS

Cu films grown on H-terminated Si(100) represent an unusual and useful system. Epitaxial growth occurs readily with little sensitivity to background pressure, deposition rate, or substrate temperature, and in spite of a 6% lattice mismatch and a rough and atomically mixed interface. These remarkable features are worthy of study in their own right, and also give the films great utility as a seed layer,[1–9] a model system for training students,[19] and a substrate for surface studies. We have determined the films' surface morphology, which is smooth on the nm scale although not on the atomic scale (rms roughness 1–2 nm) and quantified the effects of deposition rate, substrate temperature and post-deposition annealing—the smoothest films are obtained near room temperature, without annealing, at deposition rates below 3 nm/s.

For thicknesses below 5–10 nm the films consist of disconnected grains, but those grains are structurally indistinguishable from pure Cu. There is no silicide formation. The high level of surface scattering observed in electrical measurements, however, suggests that the Cu–Si interface, as well as the Cu–vacuum interface, is quite rough on the atomic scale. It remains a puzzle how such excellent and robust epitaxy is achieved in a system that departs so radically from the ideal of layer-by-layer growth. More detailed studies of film structure and composition during the initial stages of growth may help to resolve the issue.

ACKNOWLEDGMENTS

This work was supported by the National Science Foundation under Grant Nos. DMR-9201077 and DMR-9400417 (MRSEC). We thank the Center for Electron Optics of the Pesticide Research Center, Michigan State University, for the use of its AFM facility. We thank Thomas R. Bieler and Cheong Soon-Wuk, Department of Materials Science and Mechanics, Michigan State University, for their help in obtaining and analyzing the pole figures. We are grateful to R. Naik for sharing her expertise in the technique of growing

Downloaded¬21¬May¬2008¬to¬130.64.86.72.¬Redistribution¬subject¬to¬AIP¬license¬or¬copyright;¬see¬http://jap.aip.org/jap/copyright.jsp

these films, to Y. T. Cheng for his valuable advice and support, and to William Pratt for his insightful comments and suggestions.

[1] C.-A. Chang, Phys. Rev. B **42**, 11 946 (1990).
[2] C.-A. Chang, Surf. Sci. **237**, L421 (1990).
[3] C.-A. Chang, J. Appl. Phys. **68**, 5893 (1990).
[4] C.-A. Chang, J. Vac. Sci. Technol. A **8**, 3779 (1990).
[5] C.-A. Chang, J. Vac. Sci. Technol. A **9**, 98 (1991).
[6] Y.-T. Cheng, Y.-L. Chen, M. M. Karmarkar, and W.-J. Meng, Appl. Phys. Lett. **59**, 953 (1991).
[7] Y.-L. Chen and Y.-T. Cheng, Mater. Lett. **15**, 192 (1992).
[8] Y.-T. Cheng and Y.-L. Chen, Appl. Phys. Lett. **60**, 1951 (1992).
[9] R. Naik, M. Ahmad, G. L. Duifer, C. Kota, A. Poli, Ke Fang, U. Rao, and J. S. Payson, J. Magn. Magn. Mater. **121**, 60 (1993).
[10] T. Ohmi, T. Saito, T. Shibata, and T. Nitta, Appl. Phys. Lett. **52**, 2236 (1988).
[11] M. Sosnowski, H. Usui, and I. Yamada, J. Vac. Sci. Technol. A **8**, 1470 (1990).
[12] C.-A. Chang, J. Appl. Phys. **67**, 566 (1990).
[13] C.-A. Chang, J. C. Liu, and J. Angilello, Appl. Phys. Lett. **57**, 2239 (1990).
[14] B. G. Demczyk, R. Naik, G. Auner, C. Kota, and U. Rao, J. Appl. Phys. **75**, 1956 (1994).
[15] T. Takahagi, I. Nagai, I. Ishiytani, H. Kuroda, and Y. Nagasawa, J. Appl. Phys. **64**, 3516 (1988).
[16] T. Takahagi, I. Ishiytani, H. Kuroda, Y. Nagasawa, H. Ito, and S. Wakao, J. Appl. Phys. **68**, 2187 (1990).
[17] Y. J. Chabal, G. S. Higashi, K. Raghavachari, and V. A. Burrows, J. Vac. Sci. Technol. A **7**, 2104 (1989).
[18] P. Dumas, Y. J. Chabal, and G. S. Higashi, Phys. Rev. Lett. **65**, 1124 (1990).
[19] M. Longiaru, E. T. Krastev, and R. G. Tobin (unpublished).
[20] J. Yang, C. Wang, K. Tao, and Y. Fan, J. Vac. Sci. Technol. A **13**, 481 (1995).
[21] J. S. Kallend, U. F. Kocks, A. D. Rollett, and H.-R. Wenk, Mater. Sci. Eng. A **132**, 1 (1992).
[22] H.-R. Wenk, *Preferred Orientation in Deformed Metals and Rocks: An Introduction to Modern Texture Analysis* (Academic, New York, 1985).
[23] Digital Instruments Nanoscope III Scanning Probe Microscope.
[24] G. Fischer, H. Hoffmann, and J. Vancea, Phys. Rev. B **22**, 6065 (1980).
[25] A. A. Baski and H. Fuchs, Surf. Sci. **313**, 275 (1994).
[26] K. Fuchs, Proc. Cambridge Philos. Soc. **34**, 100 (1938).
[27] E. H. Sondheimer, Adv. Phys. **1**, 1 (1952).
[28] P. Wissmann, in *Surface Physics*, edited by G. Höhler, Springer Tracts in Modern Physics, Vol. 77 (Springer, New York, 1975).
[29] D. Schumacher, *Surface Scattering Experiments with Conduction Electrons*, edited by G. Höhler, Springer Tracts in Modern Physics, Vol. 128 (Springer, New York, 1993).
[30] H. Sugawara, T. Nagano, and A. Kinbara, Thin Solid Films **21**, 33 (1974).
[31] H. Sugawara, T. Nagano, K. Uozumi, and A. Kinbara, Thin Solid Films **14**, 349 (1972).
[32] J. Bass, in *Landolt–Börnstein Numerical Data and Functional Relationships in Science and Technology*, edited by K.-H. Hellwege (Springer, Berlin, 1982), Vol. 15.
[33] D. Dayal and P. Wissmann, Thin Solid Films **44**, 185 (1977), and references therein.
[34] A. F. Mayadas and M. Shatzkes, Phys. Rev. B **1**, 1382 (1970).
[35] L. J. van der Pauw, Phillips Res. Rep. **13**, 1 (1958).

Downloaded¬21¬May¬2008¬to¬130.64.86.72.¬Redistribution¬subject¬to¬AIP¬license¬or¬copyright;¬see¬http://jap.aip.org/jap/copyright.jsp